DOI: 10.1007/s12541-012-0276-z

Analysis of Lens Manufacturing with Injection Molding

Roberto Spina[1,#], Paul Walach[2], Julian Schild[2], and Christian Hopmann[2]

1 Department of Mechanics, Mathematics and Management, Politecnico di Bari, Viale Japigia 182, 70126 Bari, Italy
2 Institut für Kunststoffverarbeitung (IKV), RWTH Aachen, Pontstraße 55, 52062 Aachen, Germany
Corresponding Author / E-mail: r.spina@poliba.it, TEL: +39-80-5962768, FAX: +39-80-5962768

KEYWORDS: Injection Molding, Spherical Lenses, Optimization, Numerical Simulations.

In the present research, the authors investigated the lens manufacturing with the injection molding process by using the geometrical contour errors as the quality criterion. In order to produce functional injection-molded optical components, a special cavity mold was used to perform experimental testing for biconvex spherical lenses and numerical simulation was used to help during mimic of the process behavior. The approach was divided into validation step and optimization step. In the validation step, a reliable numerical model was designed to reproduce material features during filling and shrinkage, in order to correctly evaluate lens deflection. In the optimization step, the Grey Relational Component analysis coupled to the Taguchi Design was used to identify the optimal parameter set leading to the best values of lens total deflection, Peak-to-Valley and Root Mean Square between real and ideal lens surface geometry.

Manuscript received: October 9, 2011 / Accepted: July 3, 2012

1. Introduction

The continuous growth of international markets and globalization force plastic manufactures and suppliers to give faster responses at lower costs. While glass lenses are preferred, several applications require high quality plastics lenses in an effective way. Several researches have been carried out on analysis and manufacturing of optical plastics lenses with injection molding from the point of view of the process itself. Some authors put more attention on lens design and numerical simulations. Turng et al.[15] proposed an integrated CAE approach to optimize PMMA lens manufacturing. The objective was the shortening of the manufacturing cycle time and the quality criterion used was the decrease of optical retardation in order to evaluate induced stresses and birefringence. Pazos et al.[12] numerically estimated the effect of the lens thickness on PC biconcave and biconvex lenses, evaluating the lens quality in terms of number and positions of weld lines and air-traps. Wen and Wen[18] numerically simulated the injection molding of a PMMA aspheric lens and optimized it by using a Design of Experiments (DoE). The quality criteria used to optimize the process were the maximum value and the maximum variation of the volumetric shrinkage. Lin and Lee[6] performed the mold design analysis for a PC aspherical lens of a mobile phone camera, varying gate shape and cross-section sizes as well as different cooling circuit types. Hu et al.[3] investigated the effect of the holding pressure and gate size on the quality of a PMMA aspheric lens. The reduction of the linear shrinkage measured in specific points of the lens was used as the main quality criterion. Park and Dang pointed out the importance of cooling system in injection molding in terms of productivity and quality, as well mold-making cost. The author used conformal cooling channel with an array of baffles to achieve uniform cooling over the entire free-form surface of molded parts.

Other authors investigated the effects of the process parameter choice on geometrical and optical lens properties and features. Kim et al.[5] employed a numerical approach to study the effects of the main process parameters on optical properties of a PMMA CD-ROM lens. The optical quality was measured in terms of birefringence distribution and pattern caused by the stress-difference distribution at the mid-surface of the lens. Lu and Khim[7] carried out a statistical experimental analysis to produce a PC mono-axial spherical lens. The main process parameters investigated were the injection speed, holding pressure and mold temperature. Birefringence patterns linked to residual stress levels and contour errors were used as quality criteria. Park and Joo[11] proposed a new ray tracking method integrated into simulation software to numerical evaluate optical performances. The method allowed the distribution of the refractive index to be calculated from the injection molding simulation in order to investigate the effects of the process conditions on a PMMA lens. Michaeli and Forster[9] studied the measurement technique to control the geometrical accuracy of a PMMA aspherical lens. The authors used a scanning

measuring system employing an optical single point sensor to acquire geometries of lenses manufactured with different holding pressures and relative mold insert cavities and then to compare the results. Michaeli et al.[8] studied the geometrical accuracy and optical performance of PMMA aspherical lenses by using special sensors. A chromatic sensor was used to measure the lens geometry with a non-contact system while a Shack-Hartman sensor was involved to characterize optical properties by determining the wave front gradient in different locations. Wang and Lai[17] and then Chang et al.[2] used fully 3D numerical simulations of a COC (cyclic-olefin-copolymers) aspheric lens coupled to Design of Experiments (DoE). The quality criterion adopted was the optical birefringence while Taguchi was used as the DoE technique. Photo-elasticity measurements were carried out to confirm and support numerical predictions. Tsai et al.[14] experimentally investigated the relationship between process parameters and optical characteristics of a PMMA aspherical lens. The quality criteria were the light transmission, surface waviness and finish. Shieh et al.[13] analyzed the influence of injection molding parameters on manufacturing of large diameter PC aspherical lenses. The lens design was initially carried out with simulation software and then refined with some experimental trials supported by statistical analysis of experiments. The quality criteria were the lens birefringence and surface profile errors.

In the present research, the authors investigated the optimization of the injection molding parameters by using the geometrical contour errors of the lenses as the quality criteria. In order to produce functional injection-molded optical components, a two cavity mold with two different lens geometries (biconvex and plane-conical) was used to perform numerical simulations and experimental testing. A 3D model was initially built and then validated with some experimental trials to reproduce all phases of the injection molding, directly starting from the 3D-CAD model of the desired molded parts. The following experimental plans were performed on both numerical models and experiments with Design of Experiment approach. The main outcomes expected from this work are the identification of optimal parameters leading to the reduction of the geometrical contour errors.

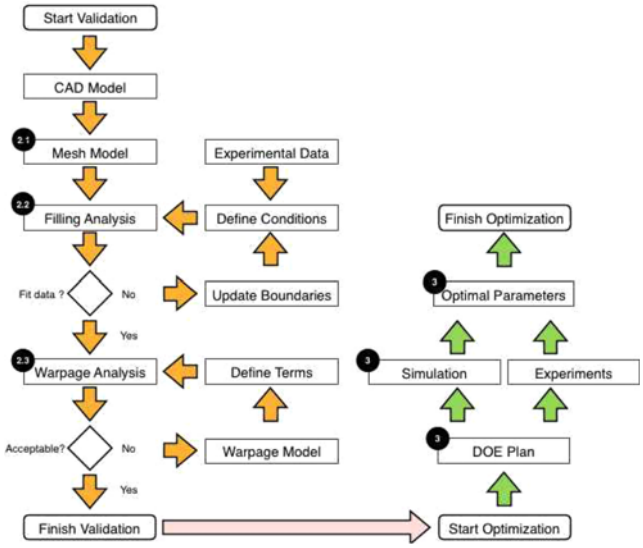

Fig. 1 Workflow

2. Simulation and Validation of FE models

The workflow employed in the present research started with the creation of reliable numerical models to simulate the injection molding process of lenses using a real designed mold followed by experimental trials needed to validate these numerical models and the subsequent combined numerical-experimental analysis to optimize the whole manufacturing process. The complete workflow is shown in Figure 1, in which the numbers inside the circles correspond to the following paragraphs.

2.1 Definition of the FE models and experimental conditions

In this study, a biconvex spherical lens and a plane-conical lens were investigated. The main radial dimension of both lenses was equal to 35 mm while the average thickness was 8 to 9 mm. A two cavity mold was used to produce both lenses with a symmetrical force flow (Figure 2). The figure also shows the mold design with the runner and gate system as well as the cavity configuration used. The CAD model was directly converted and then meshed with commercial software Autodesk® Moldflow® Insight. The mesh models were dual domain and fully 3D with tetra elements. The choice to concurrently use these mesh technologies was necessary for gaining more in-depth results respect to the single mesh technique, even if the computational effort was more intense. The number of mesh elements was high because the feeding system was meshed not using the 1D elements but the 3D elements only.

Some numerical trails were carried-out before setting the mesh grain in order to achieve a good compromise between numerical performance and solver accuracy. As a result the dual domain mesh consisted of more than 10,500 triangle elements and 5,300 nodes while the tetra mesh consisted of more than 110,000 elements and 21,000 nodes.

The polymer material was a Plexiglas 7N OQ of Evonik Röhm GmbH, an amorphous thermoplastic molding compound (PMMA) especially designed for optical parts with good flow, high mechanical strength, surface hardness, wear resistance, heat deflection temperature and light transmission. The recommended processing conditions, suggested from Evonik, were a pre-drying temperature of max 93°C for 3 hours, a melt temperature ranging from 220 to 260°C and a mold temperature ranging from 60 to 90°C. Based on this data, the process parameters used for the filling phase of the numerical simulations were the following: (i) constant velocity profile with a flow

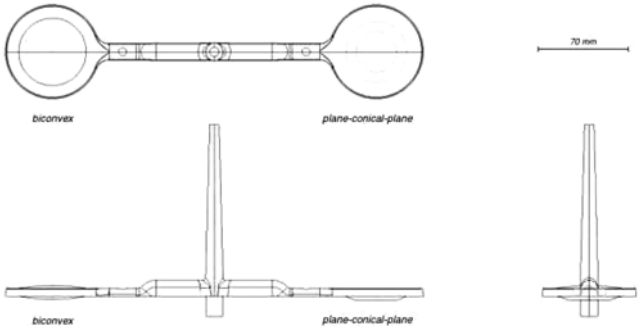

Fig. 2 CAD model

rate equal to 10 cm^3/s, (ii) velocity/pressure switch-over at 90% of volume filled, (iii) mold surface and polymer melt temperatures equal to 85ºC and 230ºC respectively. The mold is normally kept as cold as possible to minimize the cycle time for thin parts. However, manufacturing of thick lenses requires enough time to allow polymer to flow and holding pressure to be kept as long as possible (high gate-off time) to reduce shrinkage. On the contrary, the melt temperature was lower than recommended to reduce cooling time and quickly create a thick frozen layer on mold surfaces acting as thermal insulators. The holding pressure phase consisted of a 3-step profile (medium-high-low) with the maximum pressure equal to 20 MPa, applied for a total time of about 50 s from the filling/holding switch. The cooling time was set to 120 s. The detailed comparison between simulated results and actual in-process data was performed with an instrumented mold.

2.2 Filling analysis

The filling analysis, performed by using the process parameters defined above, is shown in Figure 3 from the front and top point of view. As the figure shows, the filling progression was well balanced between the two cavities because the simultaneous filling of all flow paths (right and left) at the same time was achieved. The complete filling was realized in 7.33 s. The filling progression is also shown in Figure 4 with particular attention to the biconvex spherical lens. The lens was filled from a single gate with a constant injection rate. As the melt comes out of the gate, the velocity of the flow front decreased as it diverged in a radial pattern through the increasing part volume. Upon reaching the borders, the flow was limited to only fill the last region positioned in the right side and the melt velocity rapidly increased.

The difference between the initial and final flow front velocity caused the increase of shear stress and shear rate values (Figure 5). In this case, these values were lower than the maximum allowed (0.4 MPa) for the chosen polymer, allowing the increase of process parameters such as injection speed and/or the first value of the holding pressure. The pressure values at filling/packing switch and at the end of filling, measured in the injection location point, were equal to 12.30 MPa and 12.61 MPa respectively.

The validation of the numerical simulation trials was performed by comparing the pressure-time history recorded from the pressure transducers located into specific positions of the mold cavities with the pressure data of the mesh nodes in the same positions. The Kistler direct cavity pressure temperature transducers 6189A2, characterized by a front diameter equal to 2.5 mm, were placed along the centered flow direction of the biconvex lens in points P1 and P2 (Figure 6). In this way the measurement errors relating to variations in screw shear variations and plastic composition were eliminated, allowing a better control on process parameters. The sensor P1 allowed the gate-off to be evaluated while the sensor P2 allowed a short-shot to be detected by identifying zero pressure at the end-of-cavity. These start and end-of-cavity sensors were the key for sensing short-shots and automated part containment. Data recorded from these pressure transducers was used in comparison with the simulated pressure sensors N1 and N2 located in the same positions, together with simulated pressure data at the injection location INJ. As Figure 7 points out, the FE model was in very good agreement with experimentations. The simulated sensors N1 and N2 were able to reproduce the same evolution and trend recorded of the real transducers P1 and P2. Main differences between simulated and experimental data occurred during the pressure rise simulated from sensor P1 (underestimated) at the end of the filling phase, at the maximum value of the holding pressure simulated from sensor P2 (underestimated) and during cooling (overestimated). However, these differences were sufficiently low to be considered negligible.

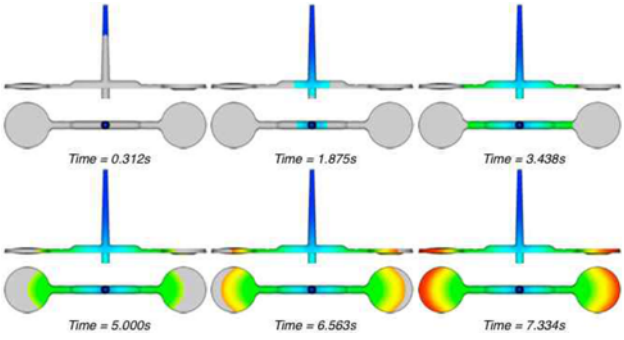

Fig. 3 CAD model

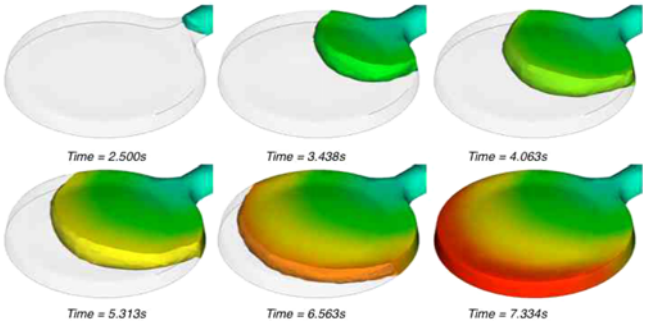

Fig. 4 Filling progression of biconvex lens

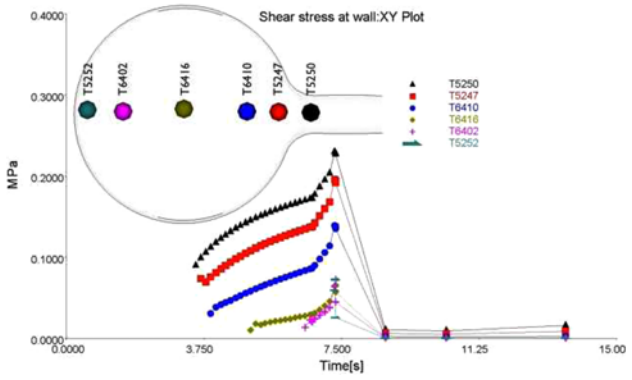

Fig. 5 Shear stress at wall of biconvex lens

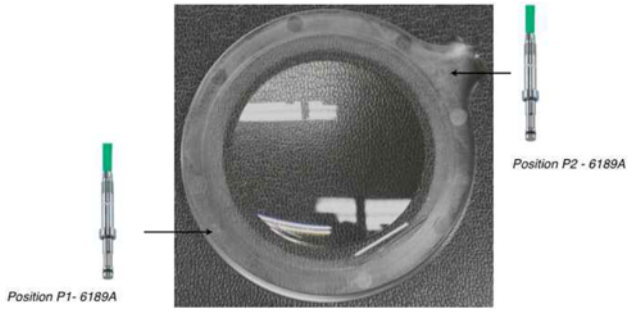

Fig. 6 Position of KISTLER pressure and temperature transducers

2.3 Warpage analysis

The warpage simulation required a more in-depth analysis. Warpage of lenses can cause significant production and reliability problems. Symptoms of adverse warpage are mainly related to geometrical distortions and aberrations since it is well known that these defects do not exist in a well-designed and well-built lens. For this reason, the objective was to achieve robust models able to give reliable distortion predictions. Lens surface topography was examined by employing the MicroGlider® system (Fries Research & Technology GmbH, Germany), a special device using chromatic aberration to illuminate the entire lens surface by focusing different wavelengths of light at different locations.

The determination of the focal point position allows the measurement of the lens height. Top and bottom surfaces were acquired with a sampling rate of 30-1000 Hz and a resolution equal to 250 points/80 mm. The scanned area was 80 mm × 80 mm with the lateral and vertical resolution ranges respectively equal to 1-2 μm and 0.01-300 μm. Figure 8 reports topographies of the top and bottom surfaces of the biconvex lens, together with its center cross sectional profiles. This data was very important as the reference for the numerical model tune-up. From the point of view of numerical simulations, the results of the flow analysis coupled to the thermal analysis were the input of the mechanical model in conjunction with the variations of the mechanical properties as a function of temperature. In order to calculate residual stresses, a generalized Voigt-Kelvin viscoelastic model with suitable material data over the range of conditions encountered in injection molding is usually required. Such a model must be valid in the melt state, during the phase change and in the solid state.

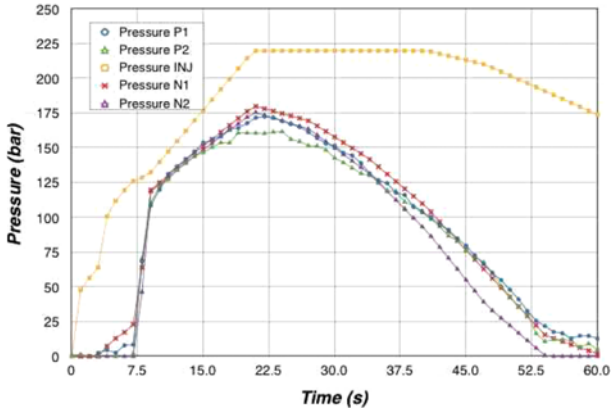

Fig. 7 Pressure history of real (P1, P2) and simulated (INJ, N1, N2) transducers

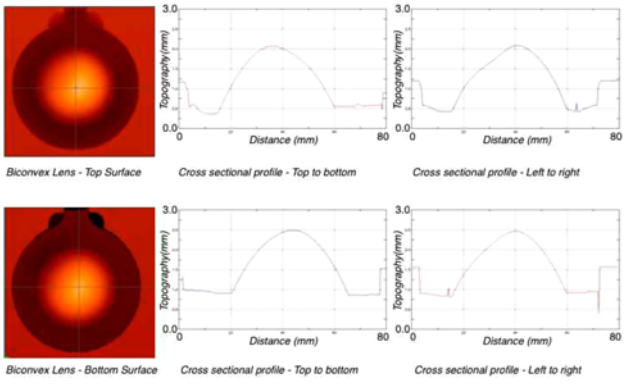

Fig. 8 Lens topography

At this time, no suitable theoretical model seems to be available to perform predictions in all temperature ranges and thus some simplifications are normally required to perform numerical simulations. The part shrinkage is obtained from the structural analysis by using the calculated residual stresses as loading conditions of the mechanical model, in conjunction with a set of additional boundary conditions to prevent the rigid body motion of the component. The results of the numerical simulations are reported in Figure 9 in terms of the total deflection of the biconvex lens. The same results are transformed into data suitable for the surface topography analysis (Figure 10) to allow the comparison with the molded lens. As the figure shows, numerical simulations underestimated the maximum value of warpage in X, Y and Z directions. A possible reason of this behavior was that the warpage model used for numerical simulations introduces simplifications leading to defective predictions.

To improve simulation accuracy, the adoption of the hybrid model proposed by Kennedy and Zheng[4] was necessary. The hybrid model used measured shrinkage data to improve numerical predictions of the theoretical models, by employing this formulation:

$$\sigma_c^{//} = b_1\sigma_p + b_2\tau + b_3 \tag{1}$$

$$\sigma_c^{\perp} = b_4\sigma_p + b_5\tau + b_6 \tag{2}$$

where $\sigma_c^{//}$ and $\sigma_c^{\perp}$ are the corrected principal stresses in the directions parallel and transverse to flow respectively, σ_p is the predicted residual stress and τ is a measure of the material orientation while the terms b_i with $i = 1...6$ are constants to identify. This procedure was very time consuming, requiring to run several computationally intensive simulations, as Cellere and Lucchetta[1] also reports. For this reason, a Design of Experiments (DOE) technique called Response Surface Method (RSM) was used to identify these constants. The terms b_i were the control variables while the total displacement of specific nodes of

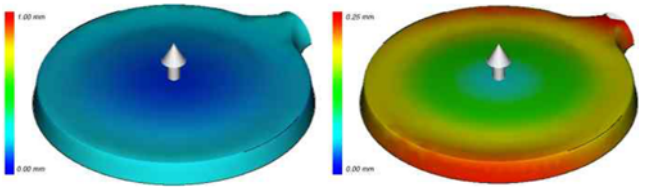

Fig. 9

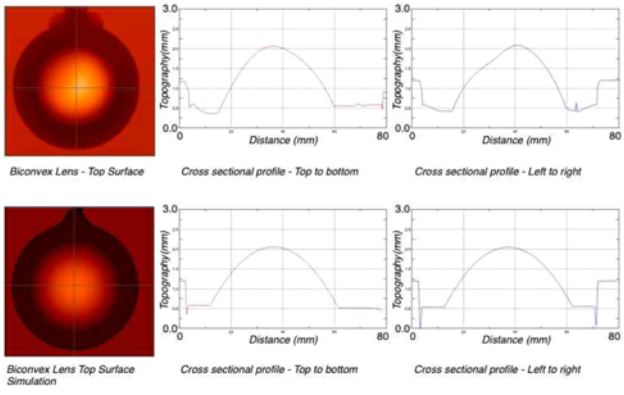

Fig. 10 Numerical and experimental topography

the numerical model were the response variables Y_i with $i = 1...3$. The choice of this technique was carried-out because RSM is normally used to evaluate interactions and even quadratic effects, therefore giving an idea of the (local) shape of surfaces associated to response variables, as Montgomery[10] suggests. Among RSM, the Box-Wilson Central Composite Design, commonly called Central Composite Design (CCD), was selected as the most appropriate. The CCD contains an embedded factorial or fractional factorial design with center points augmented with a group of star points in order to estimate curvature. Table 1 reports the minimum and maximum range values of the input variables b_i, settled on after analyzing the PMMA polymer class. The entire CCD plan for the numerical simulations consisted of 86 design runs ($|\alpha| = 6^{1/4}$). The results of the design runs are reported in Table 1 in tabular format and Figure 11 in graphical format. The response variables were the maximum deflections at the center of the top surface (Y_1), the maximum deflection along a radius parallel (Y_2) and perpendicular (Y_3) to the flow. The CCD plan correctness was witness to the fact that the corresponding real values of reflection were within the response variable ranges. Table 2-Table 4 reporting the Analysis of Variance (ANOVA) of response variables Y_1-Y_3 point out that the linear model was very significant in all responses. The coefficients of determination (R^2/adjusted R^2) of this model for the response variables Y_1, Y_2 and Y_3 were (0.8108/0.7227), (0.8811/ 0.825) and (0.8965/ 0.8423) respectively. These high values of the coefficient of determination allowed the estimation of the correct values of the control variables to associate to the real total deflections. In particular, the target values Y_i, measured from the lens topography, were (0.2, 1.0, 0.65) mm and the related constants b_i were (1.9, -0.27, 0.02, 0.3, -0.45, 0.01).

Figure 12 shows the comparison between the warpage results of the FE simulation with the viscoelastic shrinkage model (left side) and of the hybrid model (right side) with computed constants b_i.

Table 1 Central Composite Design

Factor	Low Level	High Level	Low Coded	High Coded
b_1	0.0	2.0	-1.0	1.0
b_2	-0.5	0.0	-1.0	1.0
b_3	0.0	0.1	-1.0	1.0
b_4	0.0	2.0	-1.0	1.0
b_5	-0.5	0.0	-1.0	1.0
b_6	0.0	0.1	-1.0	1.0
Response	Low Level	High Level	Mean	Std.Dev.
Y_1	0.07	1.69	0.35	0.39
Y_2	0.26	5.19	1.14	1.28
Y_3	0.26	4.40	1.23	1.32

Table 2 ANOVA of Response Y_1 (only factors with F-Value > 7)

Source	Sum of Squares	Degree of Freedom	Mean Square	F - Value	P Value
Model	10.560	27	0.390	9.21	< 0.0001
b_1	1.640	1	1.640	38.52	< 0.0001
b_4	1.630	1	1.630	38.26	< 0.0001
$b_1 \times b_3$	0.590	1	0.590	14.00	0.0004
$b_1 \oplus b_4$	2.620	1	2.620	61.68	< 0.0001
$b_1 \oplus b_6$	0.430	1	0.430	10.06	0.0024
$b_3 \oplus b_4$	0.600	1	0.600	14.09	0.0004
$b_4 \oplus b_6$	0.430	1	0.430	10.14	0.0023
$(b_1)^2$	0.310	1	0.310	7.21	0.0094
$(b_4)^2$	0.310	1	0.310	7.41	0.0085

Table 3 ANOVA of Response Y_2 (only factors with F-Value > 7)

Source	Sum of Squares	Degree of Freedom	Mean Square	F - Value	P Value
Model	124.850	27	4.620	15.92	< 0.0001
b_1	20.880	1	20.880	71.86	< 0.0001
b_3	12.980	1	12.980	44.67	< 0.0001
b_4	20.210	1	20.210	69.57	< 0.0001
$b_1 \times b_3$	11.790	1	11.790	40.58	< 0.0001
$b_1 \oplus b_4$	22.430	1	22.430	77.21	< 0.0001
$b_3 \oplus b_4$	11.790	1	11.790	40.58	< 0.0001
$(b_1)^2$	2.970	1	2.970	10.22	0.0023
$(b_4)^2$	4.080	1	4.080	14.04	0.0004

Table 4 ANOVA of Response Y_3 (only factors with F-Value > 7)

Source	Sum of Squares	Degree of Freedom	Mean Square	F - Value	P Value
Model	133.880	27	4.960	18.60	< 0.0001
b_1	27.460	1	27.460	102.99	< 0.0001
b_4	27.840	1	27.840	104.40	< 0.0001
b_6	5.270	1	5.270	19.76	< 0.0001
$b_1 \times b_3$	2.450	1	2.450	9.20	0.0036
$b_1 \oplus b_4$	29.530	1	29.530	110.74	< 0.0001
$b_1 \oplus b_6$	5.230	1	5.230	19.60	< 0.0001
$b_3 \oplus b_4$	2.450	1	2.450	9.20	0.0036
$b_4 \oplus b_6$	5.230	1	5.230	19.60	< 0.0001
$(b_1)^2$	4.770	1	4.770	17.90	< 0.0001
$(b_4)^2$	4.160	1	4.160	15.61	0.0002

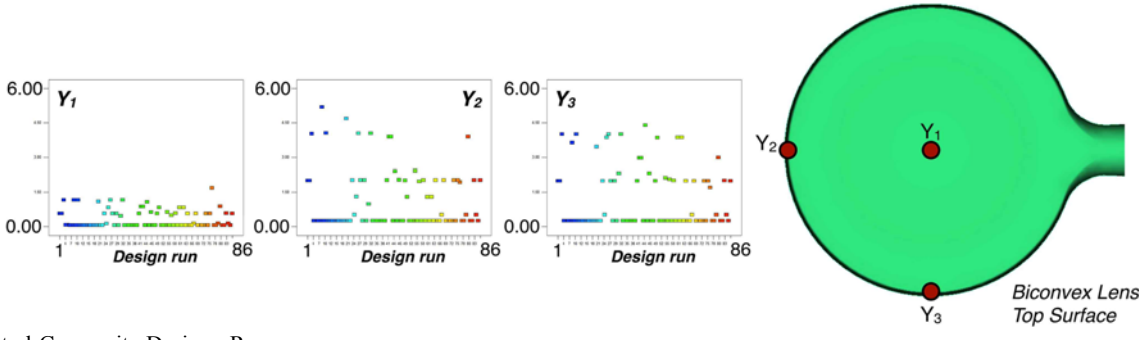

Fig. 11 Central Composite Design - Response

3. Optimization

The following phase was devoted to the process optimization. The main parameters investigated were the mold temperature T_{MOLD}, melt temperature T_{MELT}, injection flow rate Q, switch FP between velocity and pressure phase, holding pressure P and cooling time t_{COOL}. The injection flow rate, representing the evolution of the flow rate Q in function of the stroke, started with the initial value Q_{START}, linearly increased to the intermediate value Q_{GAIN}, remained at this value for about 10mm-stroke and then linearly decreased to the initial value Q_{START} (Figure 13).

The pressure profile, representing the evolution of the holding pressure P in function of time t, started 2s after the switch between filling and compression phase with the value P_{START}, linearly increased to the value P_{GAIN} during the time interval t_{GAIN}, remaining at this value for 10s and then linearly decreased to the value P_{END} during the time interval t_{END} (Figure 14). These ranges were used to design Taguchi orthogonal array plan and identify the cause of variations while selecting the optimal process parameters. The main ranges of variation of the process parameters are reported in Table 5. The response variables chosen for the optimization were the Total Deflection (TD), Peak-to-Valley (P-V) and Root Mean Square (RMS) values, selecting the criterion "Smallest is the best" for the analysis of each single response. The total number of simulation runs was equal to 12, as reported in Table 5. The response variable TD was selected to evaluate injection molding conditions, in coherence with analyses performed in the previous paragraphs, while P-V and RMS were useful to evaluate the quality of the optic.

At first glance, the response variables P-V and RMS may be considered as alternatives but the distinction between them is very important. These responses measure the difference between the actual optical surface and the expected defect-free surface. While P-V measurement has been the most common method of specifying optical system accuracy, RMS is a much better method for quantitatively measuring the quality of an optic. In more detail, the P-V is the difference between the highest and lowest parts on the surface of the optic, those top and bottom being defined as the local difference between the actual optic and the ideal one. It looks at only two points, the highest and lowest, and ignores all points lying between. As a consequence, the curvature of the optics is not took into account, making difficult to predict its performance. An optical system having a large P-V error may actually perform better than a system having a small P-V error. A more efficient measurement criterion is the RMS

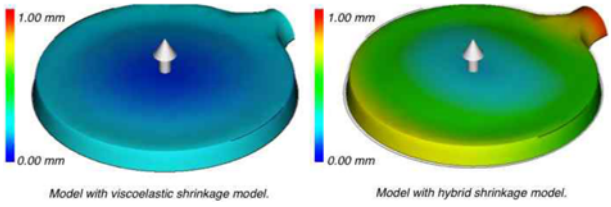

Fig. 12 Numerical warpage with hybrid shrinkage model - TD

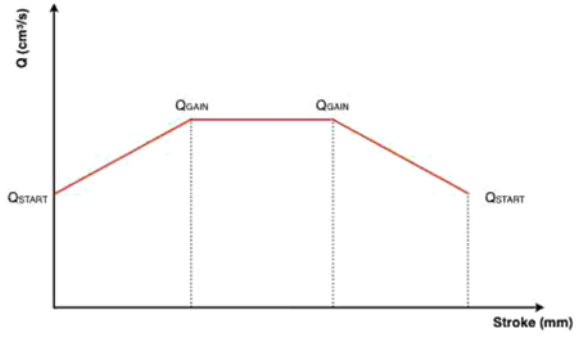

Fig. 13 Injection profile

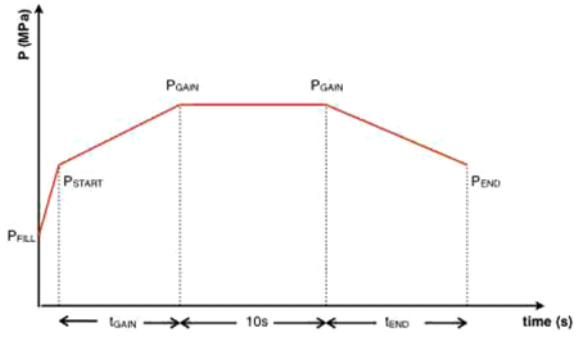

Fig. 14 Pressure profile

Table 5 Taguchi design and results

	°C	°C	cm3/s	cm3/s	MPa	MPa	MPa	s	s	s	%	mm	μm	μm
Run	A	B	C	D	E	F	G	H	I	J	K	R1	R2	R3
1	220	60	10	0	10	0	-5	10	5	100	90	1.7101	32.4826	5.4003
2	260	60	10	5	15	5	-5	20	10	100	90	1.6254	41.5456	6.2718
3	260	90	15	0	10	0	-5	20	10	100	95	1.6826	34.2748	5.6728
4	220	90	15	0	15	5	-5	20	5	200	90	1.6604	33.7082	5.8583
5	260	60	15	0	15	5	0	10	5	100	95	1.6436	45.5115	6.7473
6	220	60	10	0	10	5	0	20	10	200	95	1.7053	43.8118	6.1261
7	260	90	10	5	10	5	-5	10	5	200	95	1.6886	56.5593	8.1713
8	220	90	10	5	15	0	0	20	5	100	95	1.6792	34.0859	8.4828
9	260	60	15	5	10	0	0	20	5	200	90	1.6621	36.9187	5.6107
10	220	90	15	5	10	5	0	10	10	100	90	1.6907	32.8584	5.6275
11	260	90	10	0	15	0	0	10	10	200	90	1.6630	44.8505	6.6097
12	220	60	15	5	15	0	-5	10	10	200	95	1.6864	34.4636	8.2568

FACTOR: A = T_{MELT}, B = T_{MOLD}, C = Q_{START}, D = Q_{GAIN}, E = P_{START}, F = P_{GAIN}, G = P_{END}, H = t_{GAIN}, I = t_{END}, J = t_{COOL}, K = SWITCH, R1 = TD, R2 = P-V, R3 = RMS

value between real and ideal surfaces of the optic. This technique involves the measurement of a substantial amount of the optical surface at many points and the estimation of the standard deviation of the surface from the ideal form. This measurement has direct mathematical implications such as the possibility to calculate the Strehl ratio from it. The choice of using both criterion in the evaluation of injection molded lens was justified from the need to better understand the influence of each process parameter on final quality of the optic.

The results of the analyses are performed for Total Deflection, Peak-to-Valley and Root Mean Square values. The most important process parameters influencing the total deflection TD, in order of importance, were the starting value of the packing pressure (P_{START}), the melt temperature (T_{MELT}), the switch between filling and packing phases (FP), the maximum packing pressure (P_{GAIN}) and its time of application (t_{GAIN}), as Figure 15 shows. The increase of all above parameters, except FP switch, caused the decrease of TD while the other remaining factors had a slight influence on the TD variation. This result was in accordance with the process physics in which the polymer compressibility increased with temperature and pressure rise. The most important process parameters influencing the Peak-to-Valley values, in order of importance, were T_{MELT}, P_{GAIN}, flow rate initial value (Q_{START}), cooling time (t_{COOL}), FP and t_{GAIN} (Figure 16). The increase of T_{MELT}, P_{GAIN}, t_{COOL} and FP switch caused the increase of the P-V values as well as the decrease of Q_{START} and t_{GAIN}. The other remaining factors had a very tiny influence on the Peak-to-Valley values. This behavior can be explained by considering that the surface replication of the mold surface is unfavored by temperature increase and pressure variation during holding phase while initial fast flow-rates had positive effect. The RMS values are mostly affected, in order of importance, from FP switch, P_{START}, Q_{GAIN}, Q_{START} (Figure 17). The increase of T_{MELT}, P_{GAIN}, t_{COOL} and FP caused the increase of the RMS value as well as the decrease of Q_{START} and t_{GAIN}. The other remaining factors had a very low

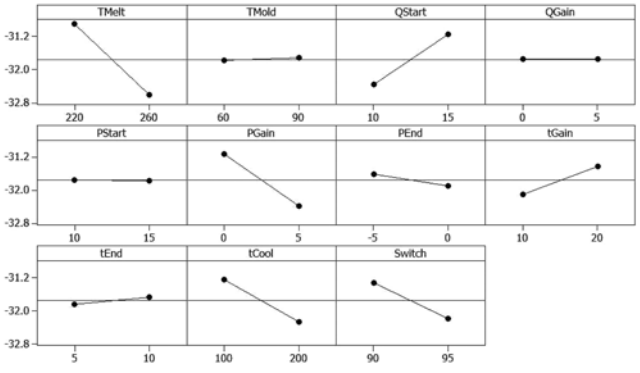

Fig. 16 Peak to Valley - Signal to Noise Plot

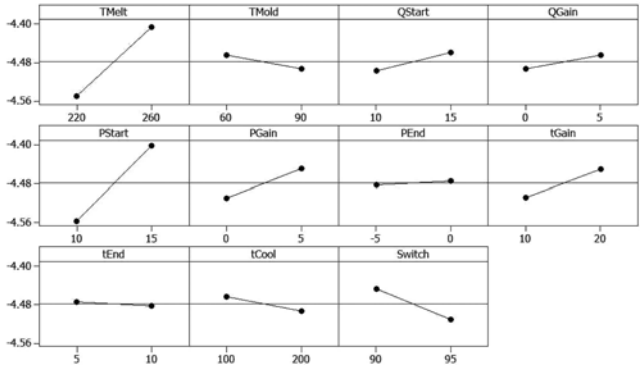

Fig. 15 Total Deflection - Signal to Noise Plot

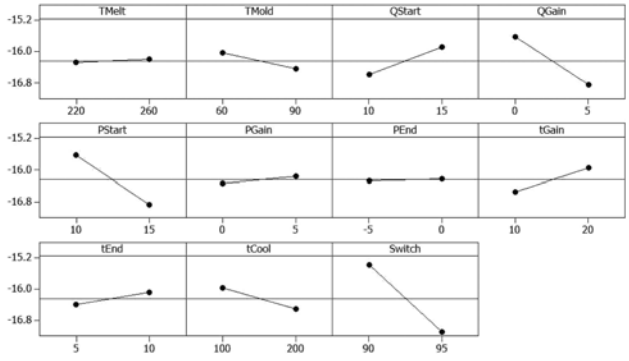

Fig. 17 RMS - Signal to Noise Plot

Table 6 Grey Relational Components

	mm	μm	μm					
Run	R1	R2	R3	SEQ1	SEQ2	SEQ3	GRG	S/N
1	1.7101	32.4826	5.4003	0.000	1.000	1.000	0.67	3.50
2	1.6254	41.5456	6.2718	1.000	0.624	0.717	0.66	3.56
3	1.6826	34.2748	5.6728	0.325	0.926	0.912	0.58	4.75
4	1.6604	33.7082	5.8583	0.587	0.949	0.851	0.62	4.14
5	1.6436	45.5115	6.7473	0.785	0.459	0.563	0.58	4.78
6	1.7053	43.8118	6.1261	0.057	0.529	0.765	0.48	6.38
7	1.6886	56.5593	8.1713	0.254	0.000	0.101	0.37	8.61
8	1.6792	34.0859	8.4828	0.365	0.933	0.000	0.48	6.45
9	1.6621	36.9187	5.6107	0.567	0.816	0.932	0.62	4.11
10	1.6907	32.8584	5.6275	0.229	0.984	0.926	0.66	3.62
11	1.6630	44.8505	6.6097	0.556	0.486	0.608	0.61	4.34
12	1.6864	34.4636	8.2568	0.280	0.918	0.073	0.46	6.76
Optimal	1.6456	29.9926	4.8556	0.762	1.103	1.177	0.86	1.43

FACTOR: R1 = TD, R2 = P-V, R3 = RMS, SEQ1 = $(TD)_n$, SEQ2 = $(P\text{-}V)_n$, SEQ3 = $(RMS)_n$

influence on the RMS value. In this case, the behavior can be justified by considering the reduction of surface replication of the mold surface was positive affected by high pressure during holding phase and sufficient holding time.

These responses were influenced by different process parameters and sometimes by the same process parameter but with opposite level value. It was possible to identify the optimal solution by selecting one response at time. For this reason, the Grey Relational Component (GRC) Analysis was applied to the Taguchi Design to convert a multiple response optimization problem into a single response optimization situation, according to Wang.[16] The objective function of this new optimization problem was the Grey Relational Grade (GRG) and the optimal parametric combination was the parameter set leading to the highest GRG. The process responses $R_i(k)$ were normalized into $SEQ_i(k)$ based on the "Smallest is the best" criterion, by using:

$$SEQ_i(k) = \frac{max_i R_i(k) - R_i(k)}{max_i R_i(k) - min_i R_i(k)} \tag{3}$$

where $R_i(k)$ is the Taguchi Response, min $R_i(k)$ is the smallest value of $R_i(k)$ for the k^{th} response, and max $R_i(k)$ is the largest value of $R_i(k)$ for the k^{th} response.

Defined the ideal sequence is $SEQ_0(k)$ with $k = 1 : 3$, the definition of Grey Relational Grade revealed the degree of relation between the ideal sequence $SEQ_0(k)$ and the evaluated sequences $SEQ_i(k)$ with $i = 1 : 12$. The Grey relational coefficient ξ_i was calculated as

$$\xi_i(k) = \frac{min_i min_k \left|SEQ_o(k) - SEQ_i(k)\right| + \psi \cdot max_i max_k \left|SEQ_o(k) - SEQ_i(k)\right|}{\left|SEQ_o(k) - SEQ_i(k)\right| + \psi \cdot max_i max_k \left|SEQ_o(k) - SEQ_i(k)\right|} \tag{4}$$

with $\Psi \in [0,1]$ the distinguishing coefficient. After averaging the Grey Relational Coefficients, the Grey Relational Grade GRG_i was computed as:

$$GRG_i = \frac{1}{n} \sum_{k=1}^{5} \xi_i(k) \tag{5}$$

The Grey Relational Grade also indicates the degree of influence that the comparability sequence could explain over the reference sequence. The results of the application of the GRC analysis are reported in Table 6.

The same table reports the Signal to Noise ratio (S/N) on the last column. The solution closer to the optimum was associated to the first factor run. Once the optimal level of the process parameters was identified, the final step was the prediction and validation of the response improvement starting from the optimal level. If the predicted and observed S/N ratio values for different responses are close to each other, the effectiveness of the optimal condition can then be ensured. The Taguchi Design was evaluated again with the same runs but with the new response associated to the Grey Relational Grade, as Figure 18 shows. The optimal parameter set identified for this new response, characterized by the highest GRC value, was $T_{MELT} = 260°C$, $T_{MOLD} = 60°C$, $Q_{START} = 15\ cm^3/s$, $Q_{GAIN} = 0\ cm^3/s$, $P_{START} = 15$ MPa, $P_{GAIN} = P_{END} = 0$ MPa, $t_{GAIN} = 20s$, $t_{END} = 10s$, $t_{COOL} = 100s$ and FP = 90%. The result of the confirmation test resulted in the improvement of about 0.11 in GRG value. The response values for this optimal set, reported in Table 6 in the row Optimal, also led to the smallest S/N ratio. The optimal set was also validated with direct experimental tests, confirming the very good prediction of the proposed methods.

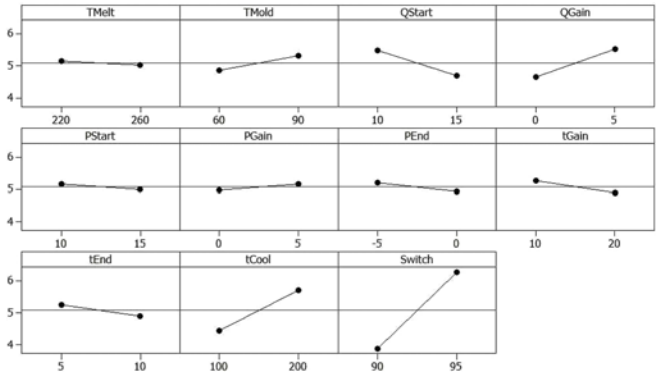

Fig. 18 RMS - Grey Relational Grade - Signal to Noise Plot

4. Conclusions

In the present research, the authors have investigated the lens manufacturing with the injection molding process by using the geometrical contour errors (lens total deflection, Peak-to-Valley and Root Mean Square between real and ideal lens surface geometry) as the quality criterion. The approach, divided into validation step for achieving reliable FE numerical models and optimization step to identify the best process parameter set, has confirmed the strength and robustness of the methods employed. In fact the numerical models have took into account the hybrid shrinkage model to predict numerical deflections very close to the real ones and support the in-depth statistical analysis for the optimization step. On the optimization side, the Grey Relational Taguchi based Component used to identify the optimal parameter sets has allowed the identification of the best performance values by simple combining the response variables and converting the multiple response optimization problem into a single response optimization situation.

From the point of view of the manufacturing results, the highest contributes to the optimal solution have been given from Root Mean Square and Peak to Valley. The Total Deflection has the tendency to be opposite to Root Mean Square and Peak to Valley, reducing the achievement of the highest lens quality. Further research will be addressed to overcome this limitation by applying the proposed methods to the injection-compression molding process.

ACKNOWLEDGEMENT

The authors wish to thank Prof. Dr.-Ing Walter Michaeli and Dr.-Ing. Markus Brinkmann of IKV - RWTH Aachen for the precious contribution in promoting cooperation among universities and supporting the research activities.

REFERENCES

1. Cellere, A. and Lucchetta, G., "Identification of CRIMS model parameters for warpage prediction in injection molding simulation," Int. J. of Material Forming, Vol. 3, No. 1, pp. 37-40, 2010.
2. Chang, Y.-J., Yu, C.-K., Chiu, H.-S., Yang, W.-H., Lai, H.-E., and Wang, P.-J., "Simulations and verifications of true 3D optical parts by injection molding process," Proc. of ANTEC, Vol. 22, No. 24, pp. 253-258, 2009.
3. Hu, G.-H. and Cui, Z.-S., "Effect of Packing Parameters and Gate Size on Shrinkage of Aspheric Lens Parts," J. of Shanghai Jiaotong Univ. (Sci.), Vol. 15, No. 1, pp. 84-87, 2010.
4. Kennedy, P. and Zheng, R., "High accuracy shrinkage and warpage prediction for injection molding," Proc. of ANTEC, Vol. 5, No. 9, pp. 1-7, 2002.
5. Kim, S. Y., Rim, M. H., Lim, W. S., and Kim, W. Y., "A Numerical Approach for Predicting the Optical Characteristics of Injection-Molded Lenses," J. of Injection Molding Technology, Vol. 4, No. 1, pp. 29-35, 2000.
6. Lin, J. C. and Lee, K. S., "Molding analysis of multi-cavity aspheric lens and mold designing," Advanced Materials Research, Vol. 83-86, pp. 77-87, 2010.
7. Lu, X. and Khim, L. S., "A statistical experimental study of the injection molding of optical lenses," J. of Materials Processing Technology, Vol. 113, No. 1-3, pp. 189-195, 2001.
8. Michaeli, W., Heßner, S., Klaiber, F., and Forster, J., "Geometrical Accuracy and Optical Performance of Injection Moulded and Injection-compression Moulded Plastic Parts," CIRP Annals - Manufacturing Technology, Vol. 56, No. 1, pp. 545-548, 2007.
9. Michaeli, W. and Forster, J., "Production of polymer lenses using injection molding," J. of Polymer Engineering, Vol. 26, No. 2-4, pp. 133-146, 2006.
10. Montgomery, D. C., "Response surface method and other other approaches to process optimization," Design and Analysis of Experiments, 5th Ed., pp. 427-510, 2000.
11. Park, K. and Joo, W., "Optical simulation of a plastic lens reflecting injection molding effects," Proc. of ANTEC, Vol. 1, No. 5, pp. 561-565, 2005.
12. Park, H.-S. and Dang, X.-P., "Optimization of conformal cooling channels with array of baffles for plastic injection mold," Int. J. Precis. Eng. Manuf., Vol. 11, No. 6, pp. 879-890, 2010.
13. Pazos, M., Baselga, J., and Bravo, J., "Limiting thickness estimation in polycarbonate lenses injection using CAE tools," J. of Materials Processing Technology, Vol. 143, No. 144, pp. 438-441, 2003.
14. Shieh, J.-Y., Wang, L., and Ke, S.-Y., "A Feasible Injection Molding Technique for the Manufacturing of Large Diameter Aspheric Plastic Lenses," Optical Review, Vol. 17, No. 4, pp. 399-403, 2010.
15. Tsai, K.-M., Hsieh, C.-Y., and Lo, W.-C., "A study of the effects of process parameters for injection molding on surface quality of optical lenses," J. of Materials Processing Technology, Vol. 209, No. 7, pp. 3469-3477, 2009.
16. Turng, L.-S., Peic, M., and Bradley, D. K., "Process Simulation and Optimization for Injection Molding-Experimental Verifications and Field Applications," J. of Injection Molding Technology, Vol. 6, No. 2, pp. 143-155, 2002.
17. Wang, C. H., "Dynamic multi-response optimization using principal component analysis and multiple criteria evaluation of the grey relation model," Int. J. of Advanced Manufacturing Technology, Vol. 5, No. 6, pp. 617-624, 2007.
18. Wang, P. J. and Lai, H. E., "Study of residual birefringence in injection molded lenses," Proc. of ANTEC, Vol. 6, No. 10, pp. 2494-2498, 2007.
19. Wen, J. and Wen, P., "The simulation and optimization of aspheric plastic lens injection molding," J. of Wuhan University of Technology (Mat. Sci.), Vol. 20, No. 2, pp. 86-89, 2005.